An ML-based approach for inverse identification of heat flux in machining

(article starts on next page)

10th CIRP Global Web Conference – Material Aspects of Manufacturing Processes

An ML-based approach for inverse identification of heat flux in machining

Ahmet Semih Erturk*,a, Amir Malakizadib, Ragnar Larssona

a Division of Materials and Computational Mechanics, Department of Industrial and Materials Science,
Chalmers University of Technology, Göteborg SE-41296, Sweden
b Division of Materials and Manufacture, Department of Industrial and Materials Science,
Chalmers University of Technology, Göteborg SE-41296, Sweden

* Corresponding author. E-mail address: erturk@chalmers.se

Abstract

This study presents an efficient and robust inverse approach to obtain the heat flux distribution on the tool rake face in oblique cutting including the tool nose radius. In this approach, Machine Learning (ML) is used to establish the relation between the parameters associated with the heat flux distribution and the error functions expressing the deviation between the embedded thermocouple measurements and Finite Element (FE) simulations. The dependency of the algorithm on the number of input data, the optimization strategy, and the overall performance of the approach are studied. The results show a clear potential of the proposed ML-based inverse identification approach.

1. Introduction

Heat generation during machining processes is a crucial factor affecting the tool wear and surface integrity of the machined components. However, the difficulties in measuring the surface temperature on the tool-chip contact area encouraged researchers either to use the analytical and numerical methods to predict the temperature rise in the cutting zone or to develop inverse approaches to estimate the heat flux on the contact area based on the experimental measurements. In the latter approach, the estimated heat flux can be applied to the models to predict the temperature under similar conditions. Numerous studies are focused on the estimation of cutting temperature and heat flux on the contact area in machining based on these approaches. For instance, numerical simulations of the chip formation process incorporating different friction models and thermal boundary conditions are widely used to obtain the temperature distribution at the tool-chip interface [1–4]. The other commonly pursued approach is to estimate the heat flux based on the classical metal cutting theories or energy methods, which is then used as a boundary condition in analytical or numerical models to obtain the temperature distribution within the tool and along the chip-tool interface [5, 6]. Combined with these modeling strategies, several authors have pursued the development of the so-called meta-models for the tool temperature prediction as the cutting or cooling-lubrication conditions vary. These studies generally exploit ML or Artificial Neural Network (ANN) models based on temperature predictions (the mean or maximum interface temperature) obtained using either of described modeling approaches [7, 8]. However, the simulation error associated with: 1) the tool-chip contact area; 2) the amount of generated heat due to the friction and plastic deformation can lead to unreliable temperature predictions at the tool-chip interface. This limits the application of these approaches for temperature predictions in cutting.

To obtain a better estimation of the heat flux and its distribution at the tool-chip interface, several studies placed their focus on the inverse heat transfer problem. These studies often use thermocouple measurements as inputs for inverse identification of the amount and/or distribution of heat flux. These approaches generally benefit from FEM (Finite Element Method) or FDM (Finite Difference Method) for simulation of the heat transfer problem, making it possible to incorporate more complex tool geometries and boundary conditions. For instance, Yvonnet et al. [9] demonstrated the potential of an FEM-based inverse ap-
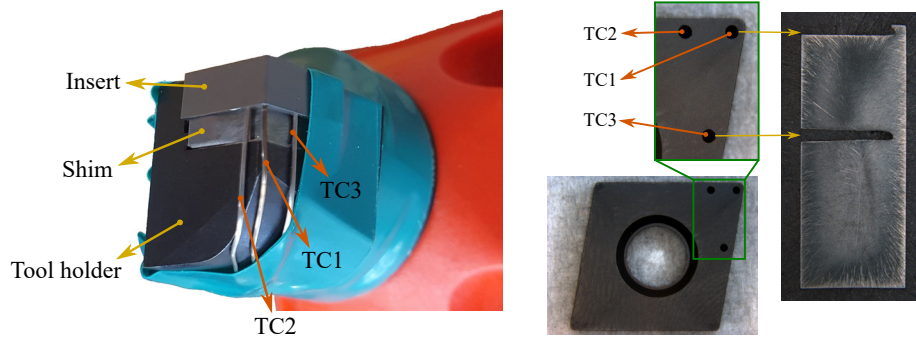
Fig. 1. Experimental setup (left) and configuration of thermocouple holes (right).

proach to obtain the heat flux distribution on the tool-chip interface and the convection coefficient of the external surfaces simultaneously. Kryzhanivskyy et al. [10] included the time-dependent heat flux distribution on the tool surface in their FE-based inverse approach. The authors evaluated the time-dependency of different heat flux expressions to determine the most suitable one giving the best match with measured temperatures. The spatial distribution of the heat flux on the rake face was also investigated using an exponential function.

In this study, we placed our focus on an accurate representation of the heat flux distribution at the tool-chip contact area. An ML-based inverse approach is developed to determine the parameters of an assumed heat flux distribution to mimic the machining. FEM is used to address the heat transfer problem and to generate the inputs required to train the appropriate ML model describing the relationship between the heat flux parameters and the absolute error between predicted temperatures and measurements at known locations. The ML model is used to obtain the optimum set of heat flux parameters giving the least error. In addition, the sensitivity of model predictions on the number of simulations required for training the ML model, the variations in the location of thermocouples, and the objective functions used for minimization are also investigated.

2. Experimental Details

Face turning (FT) experiments are performed under dry conditions on an EMCO 365 CNC lathe. The workpiece material used in the experiments is C38 steel. All machining tests are carried out on cylindrical bars with an outer diameter of $156.5mm$. The tool holder used in the experiments is C3-PCLNR-22040-12 (Sandvik Coromant). The inserts mounted on the tool holder are uncoated cemented carbide CNMA-120404-KR (Sandvik Coromant) without a chip breaker. The

insert and tool holder assembly gives 95° major cutting edge angle and 6° rake angle. Three cutting conditions (given in Table 1) are used in the experiments to investigate the effect of feed on the estimations of heat flux and temperature. The machining duration for each cut is kept short (around 4 seconds) to reduce the effect of flank and crater wear on the temperature measurements. This short machining duration would not be sufficient to reach a steady state in terms of interface temperature; however, this would not largely influence the intensity of heat flux as the tool-chip contact area and chip formation reached stable conditions during the cutting time. The experimental setup for the temperature measurements can be seen in Fig. 1. Three holes with a diameter of 0.55±0.05mm are produced using electrical discharge machining (EDM) from the bottom of the inserts with 0.6±0.2mm from the rake face of the insert. The location and the depth of the thermocouple holes were decided based on preliminary FE simulations. This was to ensure that the temperature measurements at different locations would provide sufficiently large differences required for model calibration.

Temperatures are measured with mineral insulated thermocouples (Type K), with 0.5mm diameter, embedded in the fabricated holes. A multichannel data logger is used to collect the measurements and to ensure that the measurements are synchronized. To reassess the position and depth of the holes, the flank sides of the inserts are ground after the machining tests. The grinding is continued until the holes appear, and the depths and positions are remeasured (see Fig. 1) using a stereo-optical microscope, Zeiss Discovery V20, equipped with an image processing software. The tool-chip contact areas are also measured by using Scanning Electron Microscope (SEM) after removing the built-up edge with a diluted HCl solution.

3. Heat Transfer Simulation Details

The heat transfer simulations are performed in ABAQUS. The FE models include the tool holder, insert, shim and thermocouples for a realistic representation of the experimental setup. The location and the depth of the holes and the tool-chip contact area in the FE models are defined based on the reassessed measurements. The simulations are performed for a total time of 5 seconds. A perfect contact is considered between the components of the assembly. The convection coefficient of $200W/m^2K$ is applied on the outer surfaces while the ambient temperature

Table 1. Cutting Conditions for Face Turning (FT) Experiments.

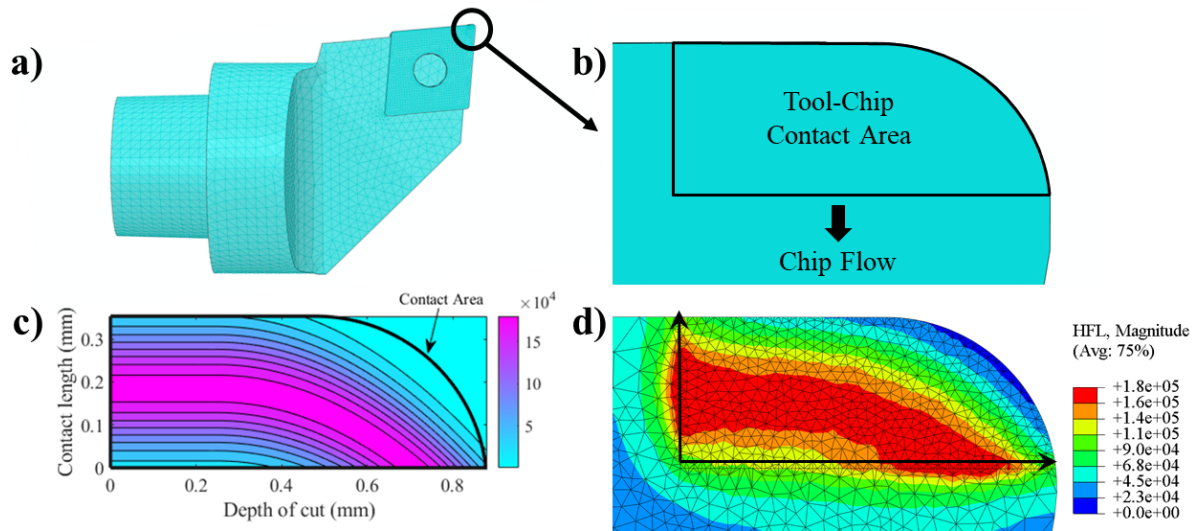| No	Cutting speed, V_c (*m/min*)	Feed, f (*mm/rev*)	Depth of cut, a_p (*mm*)
FT1	150	0.05	0.8
FT2	150	0.10	0.8
FT3	150	0.15	0.8

Fig. 2. (a) FE model, (b) tool-chip contact area, (c) heat flux (mW/mm^2) distributions obtained from ML-approach and (d) the same heat flux (mW/mm^2) applied on the tool rake face in the FE-model.

is assumed to be constant 25°C. The other boundary conditions consist of a constant 25°C at the base of the tool holder and the prescribed heat flux distribution over the tool-chip contact area (see Fig. 2).

The applied heat flux has the distribution as in Eqs. 1a and 1b. The expression given in Eq. 1a represents the effect of the tool nose radius on the heat flux while Eq. 1b is the simplified Gaussian distribution. The heat generation (or heat flux Q) due to friction is related to the shear stress and velocity ($Q \propto \tau V$). In Fig. 3, the distributions of normal stress σ, shear stress τ and velocity V are given similar to [2, 3, 5, 11]. This figure also shows the distribution of heat flux along the contact length where the heat generation due to friction and shear zones are both included similar to [1]. Gaussian distribution function given in Eq. 1b can represent this distribution well. However, it must be noted that the heat flux Q distribution needs also to be scaled to include the heat generation due to the plastic deformation in the primary shear and secondary shear zones. This can be achieved by carefully selecting the distribution parameters.

The equation of the distribution of heat flux is as follows

$$R = \begin{cases} (Y - b_2), & \text{if } X < b_1 \\ (Y - b_2) + b_3 (X - b_1)^2, & \text{if } X \geq b_1 \end{cases} \quad (1a)$$

$$Q = b_4 \exp\left(-\left(\frac{R}{b_5}\right)^2\right) \quad (1b)$$

where Q is the distributed heat flux, X and Y are coordinates, whereas $\{b_i\}_{i=1,...,5}$ are the parameters to be identified. Here, b_1, b_2, b_3, and b_5 represents the spatial distribution and b_4 represents the maximum magnitude of heat flux Q. An example of heat flux distribution obtained from ML-approach is shown in Fig. 2(c). This heat flux is then applied on the FE model on the respective surface by using the ABAQUS in-built capabilities as shown in Fig. 2(d).

The temperature readings are collected from the nodes at the top surfaces of the thermocouples, and the average temperature for each thermocouple is calculated accordingly. These values are later compared with the experimental temperature measurements at discrete time intervals to generate the inputs required for training the ML models. The material properties used for the components of the FE model are given in Table 2. The number
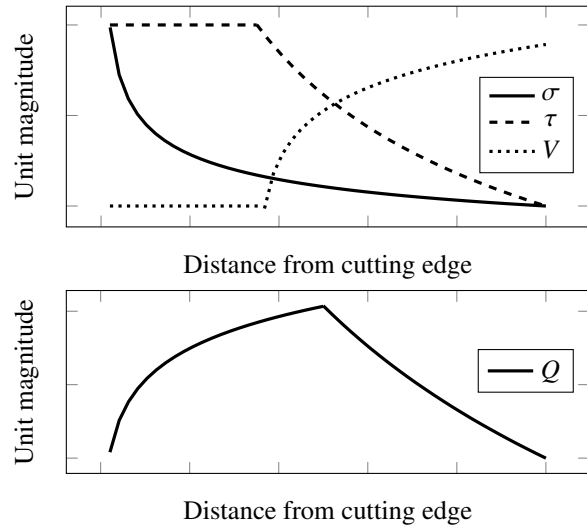

Fig. 3. Schematic distribution of normal stress, shear stress, velocity and heat generation along the contact length.

Table 2. Material Properties of the Components of FE-Model.

Component	Conductivity (W/mK)	Heat capacity (J/m^3K)
Tool holder	39.6	3.56e+6
Shim	39.6	3.56e+6
Insert	92.9	2.94e+6
Thermocouples	16.1	4e+6

of elements in FE models is selected carefully to minimize the simulation time and to ensure that the resolution of the heat flux distribution on the rake face is sufficiently high. The assembly consists of 300000 elements, and each simulation takes around 7 minutes. This is particularly important since a relatively large number of simulations need to be performed to train the ML model.

4. Inverse Identification Details

Inverse identification of the heat flux distribution is carried out using an ML-based approach. Initially, 400 sets of parameters b_1, b_2, b_3, b_4 and b_5 (in Eqs. 1a and 1b) are randomly created within certain range for each cutting condition. These ranges for the parameters b_1 to b_5 are $0 - a_p/2$, $0 - l_c$, $0 - 3$, $1e5 - 4e5$, $l_c/4 - l_c/2$, respectively, where l_c is contact length, and a_p is depth of cut. These ranges ensure that the maximum heat flux is inside the contact area and follows the edge along the nose radius properly. Then, the FE simulations are performed for all 400 heat flux distributions. In the next step, the difference between experimental and simulation temperature results is calculated for each FE simulation. Two different objective functions are defined in terms of the calculated error as follows

$$\min_{\boldsymbol{x}} \sum_n \frac{|T_{exp} - T_{sim}|}{T_{exp}} \tag{2a}$$

$$\min_{\boldsymbol{x}} \sum_n \|T_{exp} - T_{sim}\| \tag{2b}$$

where T_{exp} and T_{sim} are the experimental and simulated temperatures at discrete time instants n while $\boldsymbol{x} = \{b_i\}_{i=1,...,5}$. Eq. 2a considers the absolute percentage error between the experimental and simulated temperature at given time instants, while Eq. 2b represents the norm of the error.

The inputs parameters in Eqs. 1a and 1b and the calculated errors based on Eqs. 2a and 2b are used for building the ML model, which describes the relationship between the heat flux distribution and deviations between the experimental and simulated temperatures at discrete time instants. Such a relationship is obtained for all three thermocouple measurements. The error, which is estimated by the ML model, is then minimized to determine the optimum set of parameters for the heat flux distribution. This inverse approach is implemented in MATLAB. The Gaussian process regression, Bayesian optimization and minimization algorithm with MultiStart are used to obtain the optimum set of parameters. Cross-validation is also included in the regression model to prevent overfitting. To assess the reliability (R) of the presented inverse identification approach, an FE simulation is performed using the optimum set of parameters. The results from this simulation are compared with the experimental measurements and the error values based on Eqs. 2a and 2b are evaluated. The comparison between these values and those estimated by the ML model enables the assessment of the reliability (R) of the ML model.

5. Results

5.1. Sensitivity assessment

In this section, the performance of the ML-based inverse identification of heat flux distribution for cutting condition FT2 is evaluated using 7 different scenarios described in Table 3. In scenarios 1 to 3, the data from the thermocouples TC1 to TC3 are used to build the ML models separately. These cases are created to test the performance of the ML model. As evident from Fig. 4, the FE simulations can only capture the trends of temperature rise. This observation is expected as the time-dependency of the heat flux is not included in this investigation, however other factors could also play a role. The sensitivity of the simulation results to the position of embedded thermocouples is evaluated by changing their distance from the rake surface (i.e. by changing the depth of the holes) within a $\pm 200 \mu m$ range as depicted by the shaded regions in Fig. 4. As can be seen, the sensitivity of the results depends on how close the thermocouples are to the heat source (i.e., tool-chip contact area). TC1 temperature results span with a $50°C$ range, while TC2 and TC3 temperature measurements slightly change for the given variation in the depth of the holes (around $1°C$ and $0.2°C$, respectively).

Scenarios 4 to 7 are performed to investigate how the exclusion of the initial stage of temperature rise (i.e., 0<t<1sec), the number of the input data (FE simulations) to train the ML model and the choice of objective function influence the coefficient of determination (R^2) and the reliability (R) of model predictions. The initial rapid increase in the temperature measurements is excluded to obtain the objective functions in scenario 5. Thus, a better fit (Ave.Diff.=20.5%, R=96%) for the temperature after the initial increase is obtained compared to scenario 4. When the number of FE simulations is decreased from 400 (scenario 4) to 200 (scenario 6), the reliability (R) drops from 95% to 87% with an increase in the average difference from 23.2% to 33.4%. For better reliability with less computational time, the number of simulations can be selected between 200-400. Scenario 7 with Eq. 2b as the objective function yields almost the same average difference (23.3%) as scenario 4 (23.2%). However, the reliability of the ML model decreased to 86%. Since the main objective of the study is to represent the heat flux distribution realistically, it is crucial to have a reliable model. Thus, scenario 5 seems to be the most suitable strategy with the highest reliability and the lowest average deviation with the experimental temperature data.

5.2. Results for different cutting conditions

As discussed earlier, scenario 5 leads to the most reliable estimations. However, as reported in previous studies [10, 12, 13], the uncertainty in temperature measurements increases when the thermocouples are located near the regions with steep temperature gradients. This uncertainty reduces the reliability of the experimental data acquired from TC1 for inverse identification of the optimum set of parameters. Hence, the TC1 temperature measurements were excluded during the optimization

Table 3. Assessed Scenarios for Inverse Identification of Heat Flux Distribution of FT2.

No	Included data	Included range	Number of data	Obj. func.	R^2	Reliability	Average difference
1	TC1	0<t<4sec	400	Eq. 2a	0.99	-	-
2	TC2	0<t<4sec	400	Eq. 2a	0.99	-	-
3	TC3	0<t<4sec	400	Eq. 2a	0.99	-	-
4	All	0<t<4sec	400	Eq. 2a	0.99	95%	23.2%
5	All	1<t<4sec	400	Eq. 2a	0.99	96%	20.5%
6	All	0<t<4sec	200	Eq. 2a	0.72 ±0.27	87%	33.4%
7	All	0<t<4sec	400	Eq. 2b	0.99	86%	23.3%

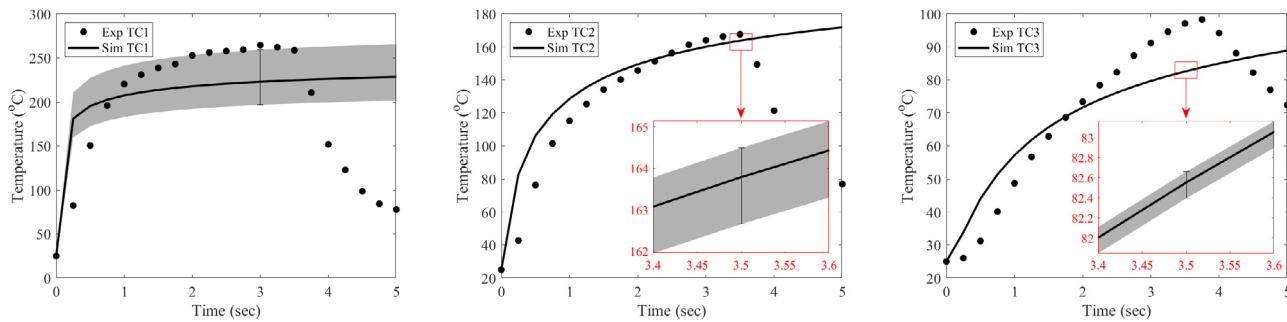*Reliability is the percentage comparison of the estimated error by ML and the error from FE simulations.

Fig. 4. Time-temperature response of scenarios 1 (left), 2 (middle) and 3 (right) simulation and experimental measurements for FT2.

process. The results of the FE simulation performed using the optimum set of parameters are presented in Fig. 5. Increasing feed from FT1 to FT3 increases the experimental temperature measurements recorded from all three thermocouples. A similar trend is observed in the simulated temperatures, i.e. an increase in feed results in an increased maximum temperature obtained from the FE simulations. However, the simulation results for TC1 show large deviations from the experimental results. This is perhaps due to the experimental uncertainties and the assumptions made for the simplicity in the simulations. Yet the estimations for TC2 and TC3 capture the overall trends of the experimental measurements with the average difference of 7.46%, 11.56% and 7.29% for FT1 to FT3, respectively. Nevertheless, the simulated maximum temperatures are larger than those reported in the literature for the similar range of cutting conditions [14], but the mean temperatures seem to be within reasonable ranges.

These large deviations between the measured and simulated temperatures are associated with a number of factors including uncertainties during experimental measurements, the assumptions made to build the FE models, and the inverse identification methodology itself. For instance, difficulties regarding the fixation of the thermocouples during the experiments may affect the contact region between the tool and the thermocouples, and therefore the temperature measurements. Using a thermal paste may results in a better contact between the surfaces, however the thermal paste should be apply carefully so that it does not introduce a gap between the surface of the holes and the tip of the thermocouples. Moreover, a thermal paste with a suitable operating temperature needs to be selected based on estimated temperature levels for the machining operation, since the prop-

erties of the paste change outside of the operating temperature. Here, no thermal paste is used to avoid the complications mentioned above, as a priori knowledge of the maximum machining temperatures was not available. However, in order to ensure the contact between the hole inner surface and the thermocouple is maintained during machining process, the dimensions of the holes and thermocouples are carefully selected, and the thermocouples are bent to create a preload toward the holes (providing the springback effects). Despite these considerations, it is still difficult to be sure how deep the thermocouples were located in the holes during machining, even though the depths of the thermocouple holes are measured by grinding the flank surfaces of the inserts after machining (due to irregular geometries at the end of the holes). This effect is investigated by considering a tolerance of $200\mu m$ for the depth and assessing the sensitivity of the results (see Fig. 4) for FT2. Moreover, the contact area is assumed to be a rectangular area over the rake face for the simplicity in this study; however, it is known that the contact area has a more complex shape in practice due to the geometry of the insert and the cutting conditions as such in [15].

As the simulation uncertainties are concerned, the function selected for the heat flux distribution is crucial for obtaining realistic results. In addition, the resolution of the heat flux distribution applied to FE simulations is proportional to the number of elements used in the contact area which can affect the estimated results. The reason is that the distribution in ABAQUS is defined as an expression based on the coordinate of the nodes in the contact area. It is worth mentioning again that, the time-dependency of the heat flux is not included in this study; however, it has a significant effect on the temperature increase rate, especially at the beginning of the readings. Thus, the exact tem-
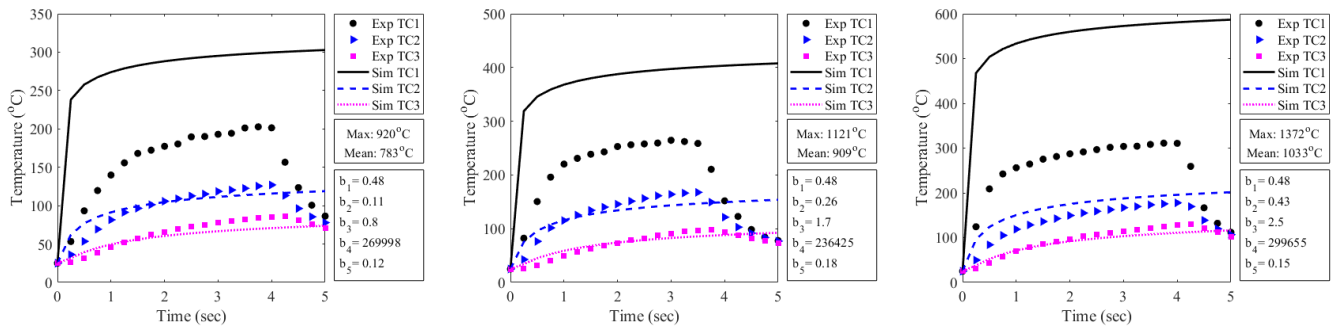
Fig. 5. The experimental and estimated time-temperature responses, heat flux distribution parameters, and the maximum and mean temperatures on the rake face. The mean temperature is the average of nodal temperatures on the tool-chip contact area. FT1 (left), FT2 (middle) and FT3 (right).

perature increase cannot be captured by FE simulations in Figs. 4 and 5. Furthermore, including the temperature-dependent material properties may also affect the results. However, some preliminary results showed that this effect is negligible for the materials used in this study. Moreover, the selected objective function and the number of data used in the ML model can affect the optimization process and so the identified set of parameters. It must be remembered that a unique solution does not exist as many optimum sets can satisfy the objective function during the optimization. Thus, different sets of upper and lower limits imposed on each parameter during the minimization process may yield different optimum sets of parameters. This suggests that these limits need to be decided carefully.

6. Conclusion

In summary, the parameters of any given heat flux distribution can be identified by using the proposed ML-based inverse approach. The sensitivities and the uncertainties of the identification process, experimentation and simulations are evaluated and discussed in this study. The results show that the proposed ML-based approach has the potential to be used for the identification of heat flux parameters. However, the results and the reliability of this approach can be improved with modifications such as a more realistic representation of contact area, time-dependency of the heat flux and spatial-dependency of maximum heat intensity with respect to the undeformed chip thickness. These factors remain to be investigated in the future.

References

[1] Li, X., Kopalinsky, E.M., Oxley, P.L.B., 1995. A Numerical Method for Determining Temperature Distributions in Machining with Coolant Part 2: Calculation Method and Results. Proceedings of the Institution of Mechanical Engineers Part B: Journal of Engineering Manufacture 209, 45–52.

[2] Dogu, Y., Aslan, E., Camuscu, N., 2006. A Numerical Model to Determine Temperature Distribution in Orthogonal Metal Cutting. Journal of Materials Processing Technology 171, 1–9.

[3] Shi, B., Attia, H., 2009. Modeling the Thermal and Tribological Processes at the Tool-Chip Interface in Machining. Machining Science and Technology 13, 210–226.

[4] Xia, Q., Gillespie, D.R.H., 2020. Quasi-static Finite Element Modelling of Thermal Distribution and Heat Partitioning for the Multi-Component System of High Speed Metal Cutting. Journal of Materials Processing Tech. 275, 116389.

[5] Usui, E., Shirakashi, T., Kitagawa, T., 1978. Analytical Prediction of Three Dimensional Cutting Process Part 3: Cutting Temperature and Crater Wear of Carbide Tool. Journal of Engineering for Industry 100, 236–243.

[6] Usui , E., Shirakashi , T., Kitagawa, T., 1984. Analytical Prediction of Cutting Tool Wear. Wear 100, 129–151.

[7] Kara, F., Aslantas, K., Cicek, A., 2016. Prediction of Cutting Temperature in Orthogonal Machining of AISI 316L Using Artificial Neural Network. Applied Soft Computing 38, 64--74.

[8] Hashemitaheri, M., Mekarthy, S.M.R., Cherukuri, H., 2020. Prediction of Specific Cutting Forces and Maximum Tool Temperatures in Orthogonal Machining by Support Vector and Gaussian Process Regression Methods. Procedia Manufacturing 48, 1000-1008.

[9] Yvonnet, J., Umbrello, D., Chinesta, F., Micari F., 2006. A Simple Inverse Procedure to Determine Heat Flux on the Tool in Orthogonal Cutting. International Journal of Machine Tools and Manufacture 46, 820–827.

[10] Kryzhanivskyy, V., Bushlya, V., Gutnichenko, O., M'Saoubi, R., Ståhl, J.E., 2018. Heat Flux in Metal Cutting: Experiment, Model, and Comparative Analysis. International Journal of Machine Tools and Manufacture 134, 81–97.

[11] Malakizadi, A., Hosseinkhani, K., Mariano, E., Ng, E., Prete, A.D., Nyborg, L., 2017. Influence of friction models on FE simulation results of orthogonal cutting process. The International Journal of Advanced Manufacturing Technology 88, 3217–3232.

[12] Attia, M.H., Kops, L., 2004. A New Approach to Cutting Temperature Prediction Considering the Thermal Constriction Phenomenon in Multi-Layer Coated Tools. CIRP Ann. - Manuf. Technol. 53, 47—52.

[13] Dour, G., Dargusch, M., Davidson, C., 2006. Recommendations and Guidelines for the Performance of Accurate Heat Transfer Measurements in Rapid Forming Processes. Int. J. Heat Mass Tran. 49, 1773--1789.

[14] Saez-de-Buruaga, M., Aristimuno, P., Soler, D., D'Eramo, E., Roth, A., Arrazola, P.J., 2019. Microstructure based flow stress model to predict machinability in ferrite–pearlite steels. CIRP Annals 68, 49-52.

[15] Attanasio, A., Ceretti, E., Fiorentino, A., Cappellini, C., Giardini, C., 2010. Investigation and FEM-Based Simulation of Tool Wear in Turning Operations With Uncoated Carbide Tools. Wear 269, 344--350.